Performance of fast-ion loss diagnostic on EAST

メタデータ	言語: English 出版者: 公開日: 2023-02-06 キーワード (Ja): キーワード (En): 作成者: WU, ChengRui, HUANG, J., CHANG, Jiafeng, ZHANG, J., ZHOU, Ruijie, XU, Z., GAO, W., ISOBE, Mitsutaka, OGAWA, Kunihiro, LIN, S. Y., HU, Liqun, LI, J. G., EAST Team メールアドレス: 所属:
URL	http://hdl.handle.net/10655/00013546

This work is licensed under a Creative Commons Attribution 3.0 International License.

Review of Scientific Instruments

Performance of fast-ion loss diagnostic on EAST

Cite as: Rev. Sci. Instrum. **89**, 10I144 (2018); https://doi.org/10.1063/1.5038782
Submitted: 05 May 2018 • Accepted: 05 September 2018 • Published Online: 19 October 2018

C. R. Wu, J. Huang, J. F. Chang, et al.

COLLECTIONS

Paper published as part of the special topic on Proceedings of the 22nd Topical Conference on High-Temperature Plasma Diagnostics

View Online Export Citation CrossMark

ARTICLES YOU MAY BE INTERESTED IN

Scintillator-based fast ion loss measurements in the EAST
Review of Scientific Instruments **87**, 11E728 (2016); https://doi.org/10.1063/1.4962245

Scintillator based detector for fast-ion losses induced by magnetohydrodynamic instabilities in the ASDEX upgrade tokamak
Review of Scientific Instruments **80**, 053503 (2009); https://doi.org/10.1063/1.3121543

Fast ion D-alpha measurements using a bandpass-filtered system on EAST
Review of Scientific Instruments **89**, 10D121 (2018); https://doi.org/10.1063/1.5038828

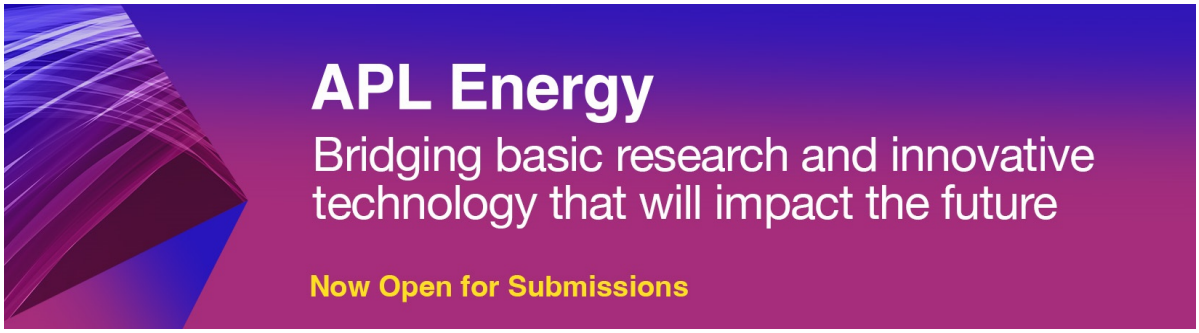

AIP Publishing

© 2018 Author(s).

REVIEW OF SCIENTIFIC INSTRUMENTS **89**, 10I144 (2018)

Performance of fast-ion loss diagnostic on EAST

C. R. Wu,[1,2] J. Huang,[1] J. F. Chang,[1,a)] J. Zhang,[1,2] R. J. Zhou,[1] Z. Xu,[3,4] W. Gao,[1] M. Isobe,[5,6] K. Ogawa,[5,6] S. Y. Lin,[1] L. Q. Hu,[1] J. G. Li,[1] and EAST Team[1,b)]
[1]*Institute of Plasma Physics, Chinese Academy of Sciences, P.O. Box 1126, 230031 Hefei, Anhui, China*
[2]*Science Island Branch of Graduate School, University of Science and Technology of China, 230031 Hefei, Anhui, China*
[3]*Advanced Energy Research Center, Shenzhen University, Shenzhen 518060, People's Republic of China*
[4]*Key Laboratory of Optoelectronic Devices and Systems of Ministry of Education and Guangdong Province, College of Optoelectronic Engineering, Shenzhen University, Shenzhen 518060, People's Republic of China*
[5]*National Institute for Fusion Science, 322-6 Oroshi-cho, Toki 509-5259, Japan*
[6]*SOKENDAI (The Graduate University for Advanced Studies), 322-6 Oroshi-cho, Toki 509-5292, Japan*

(Presented 16 April 2018; received 5 May 2018; accepted 5 September 2018; published online 19 October 2018)

The scintillator-based detector for fast-ion loss measurements has been installed on EAST. To obtain high temporal resolution for fast-ion loss diagnostics, fast photomultiplier tube systems have been developed which can supply the complementary measurements to the previous image system with good energy and pitch resolution by using a CCD camera. By applying the rotatable platform, the prompt losses of beam-ions can be measured in normal and reverse magnetic field. The thick-target bremsstrahlung occurring in the stainless steel shield with energetic electrons can produce X-rays, which will strike on the scintillator based detector. To understand this interference on fast-ion loss signals, the effects of energetic electrons on the scintillator-based detector are studied, including runaway electrons in the plasma ramping-up phase and fast electrons accelerated by the lower hybrid wave. *Published by AIP Publishing.* https://doi.org/10.1063/1.5038782

I. INTRODUCTION

Energetic particle loss is one of the most critical issues for ITER and CFETR future reactors because the lost fast-ions can reduce the lifetime of plasma facing components and also present a serious threat to machine safety. The asymmetry magnetic fields (e.g., toroidal magnetic field ripples, perturbation coils, etc.) and magnetohydrodynamic (MHD) fluctuations can cause fast-ion loss. One kind of magnetic spectrometer named as Fast-Ion Loss Detector (FILD)[1] is often used to study the effects of MHD and fast-ion-driven instabilities on fast-ion transport, which has been applied on many devices such as TFTR,[2] W7-AS,[3] NSTX,[4] JET,[5] ASDEX-Upgrade,[1] LHD,[6] DIII-D,[7] KSTAR,[8] and HL-2A.[9]

In EAST, with the improvement of auxiliary heating and current driving capacity, the physics related fast-ions become more crucial for achieving the scientific objectives such as long-pulse and high-performance discharges. A FILD system has been installed in EAST and upgraded recently.[10–12] This FILD system comprises two subsystems. One is the CCD camera system characterized by good energy and pitch resolution, and the other is the new-built photomultiplier tube (PMT) system characterized by high temporal resolution. This FILD system not only can detect lost fast-ions but also can catch the signals of energetic electrons, such as runaway electrons and fast electrons accelerated by the lower hybrid wave (LHW). The critical energy of runaway electrons is about 300 keV typically in EAST.[13] The thick-target bremsstrahlung effect caused by the interaction of energetic electrons and stainless steel shield can produce X-ray, and then the X-ray strikes on the scintillator screen and twinkle signals. This paper will present the performance of the FILD and the effect of energetic electrons on FILD measurements. In this paper, the FILD diagnostic will be shown in Sec. II. Section III will present the application of FILDs in the condition of normal and reverse magnetic field. Section IV will describe the effect of energetic electrons on FILDs. A summary will be given in Sec. V.

II. THE FAST-ION LOSS DIAGNOSTIC LAYOUT

A reciprocating FILD is installed above the outer midplane on EAST Port J, as shown in Fig. 1(a), and the FILD diagnostic is composed of the detector head, the exchange box, the optical splitter, the detection/data acquisition system, and the long shaft system. This detector can be inserted through the first wall tiles to the position just outside the last closed flux surface (LCFS). The migration length of the long shaft system covers more than 2 m, which allows the detection of fast-ion losses over a large range of phase space. The detector head can move in two dimensions. One is along the radial direction in order to adjust the radial position (1 mm of the precision) according to the plasma shape, heating power, and so on. The other is around the shaft by a rotatable platform depending on the direction of the magnetic field. A stainless steel shield with a thickness of 3 mm is used to protect the detector from the heat loads of plasma and beam ions. The scintillator screen with a size of 4 cm × 4 cm is mounted on the back-side of

Note: Paper published as part of the Proceedings of the 22nd Topical Conference on High-Temperature Plasma Diagnostics, San Diego, California, April 2018.
a)Electronic mail: changjiaf@ipp.ac.cn
b)See the Appendix of B. N. Wan *et al.*, Nucl. Fusion **55**, 104015 (2015).

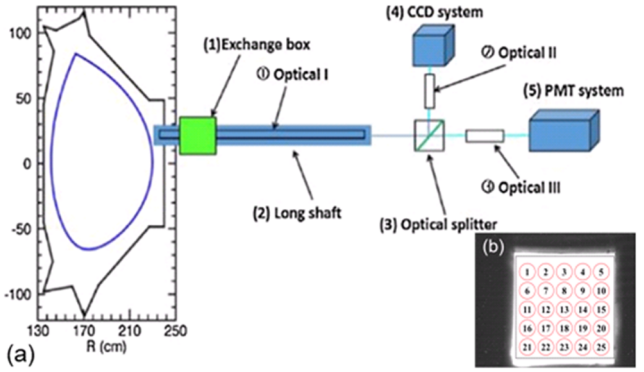

FIG. 1. An overview of the fast-ion loss diagnostic. (a) The cross section of EAST and the layout of FILD (including detector head, lenses groups, CCD camera, optical fibers, and PMTs). (b) The correspondence between the interest regions of scintillator in CCD sight field (the white region) and the alignment of the fiber array to the PMTs (25 red circles).

stainless steel shield and can be viewed through a vacuum window at the rear of the detector. Both co- and counter-rotating fast-ion losses can be measured simultaneously, for the aperture is located at the centre of collimator. Collimated by the head aperture, the escaping ions enter the scintillator chamber and inspire a light pattern on the scintillator screen. Transferred through the exchange box, the long shaft system, and the optical splitter, the light pattern is projected to a charge coupled device (CCD) camera (Phantom V2010-96GB camera) and photomultiplier tubes (PMTs, Hamamatsu Photonics, H10492-003) simultaneously. The camera can measure lost fast-ions with the pitch angle from 50° to 90° or −50° to −90° and the gyroradius from 10 mm to 180 mm. 25 channels of the PMTs with the sampling rate up to 2 MHz are applied to study the effect of instabilities on lost fast-ions in detail. One image of the CCD camera is shown in Fig. 1(b). The white region is the scintillator surface in the CCD image, and the red circles represent the 25 fibres on the scintillator which divide the scintillator into 5 × 5 array. In standard field discharges with co-current neutral beams, the lost fast-ions travel to the region of fibres 6 and 7 which are defined as **Active**. The other fibres are defined as **Passive**. In this context, the fibre 7 is chosen as **Active** and fibre 20 as **Passive**.

III. FAST-ION LOSS MEASUREMENTS IN NORMAL AND REVERSE MAGNETIC FIELD

In the standard EAST operating regimes, the plasma current Ip is directed counterclockwise from the top view. Here, the normal magnetic field (nor-B_t) is defined as clockwise viewing from the top, according to the ion B-drift directed to the lower divertor, the reverse magnetic field (rev-B_t) direction is counterclockwise, correspondingly. Figure 2 is derived from the camera of the FILD; it is shown that large first orbit losses are observed in the discharge with the counter-current neutral beam left source (named NBI2L) from port F in condition of nor-B_t (2.2 T) and rev-B_t (2.2 T), respectively. The red and yellow lines on the CCD images mesh the lost fast-ion pitch angle and gyroradius determined by the detector geometry, the aperture location, and the magnetic equilibrium. The light pattern on the scintillator shows that the pitch angle

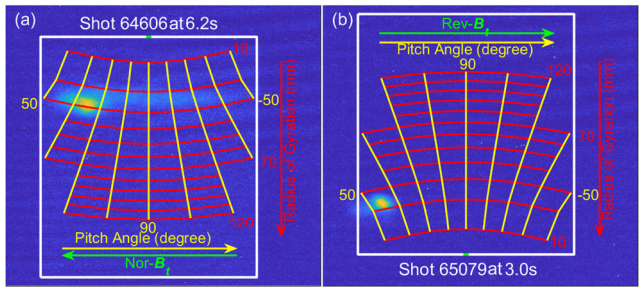

FIG. 2. Scintillator image captured by using the CCD camera in nor- and rev-B_t in discharges with the counter-current neutral beam left source (named NBI2L). The beam energy of shots 64606 and 65079 is 50 keV and 45 keV, respectively.

is 65° and the gyroradius is 30 mm for first orbit losses from the NBI2L (50 keV) neutral beam with nor-B_t in Fig. 2(a). The detector head was turned around to collect FILD signals in the rev-B_t case, and the result is shown in Fig. 2(b). The gyroradius of 20 mm and pitch-angle of 55° are manifested in the CCD camera for first orbit losses in NBI2L (45 keV) neutral beam discharge with rev-B_t. The orbit of the lost ion can be deduced further according to the energy and pitch-angle measured by using the FILD, which will be performed in the further study.

IV. EFFECT OF ENERGETIC ELECTRONS ON FAST-ION LOSS SIGNALS

A. Impact of runaway electrons on scintillator based detector

Runaway electrons are very sensitive to loop voltage, and the loop voltage changes greatly during the ramping-up of the plasma current. Figure 3 shows the waveforms of discharges 63333 and 63348 at the ramping-up phase. These two shots

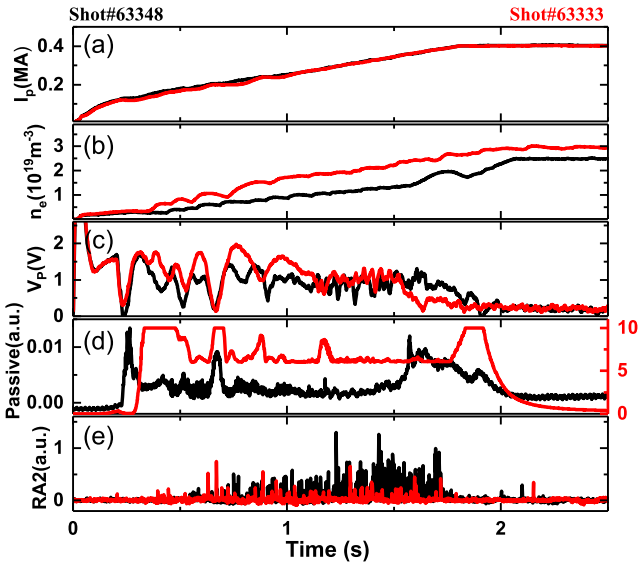

FIG. 3. Scintillator screen signal caused by runaway elections during the plasma current ramping-up: (a) plasma current, (b) line integrated electron density, (c) the loop voltage, (d) the background signals of FILD [defined as **Passive**, represented by fiber 20, as shown in Fig. 1(b)], and (e) the runaway electron signals. The position of the detector in shot 63333 is much closer to the plasma comparing with shot 63348 for about 65 mm.

have nearly the same parameters and no neutral beam injected, expect for the positions of detector are different. The detector positions at the major radius are R = 2.298 m in discharge 63333 and R = 2.363 m in discharge 63348. The plasma current ramps up to 400 kA in 1.8 s in both discharges, as shown in Fig. 3(a). During the ramping-up phase, the line integrated electron density keeps increasing [Fig. 3(b)], the loop voltage maintains at a relatively high value [around 1 V, as shown in Fig. 3(c)], and the runaway electrons emerge simultaneously [Fig. 3(e)]. As the detector of FILD is close to the plasma in the main vacuum, runaway electrons hit the stainless steel shield and the thick-target bremsstrahlung effect happens which produces X-ray. The ZnS:Ag scintillator screen located just behind the steel shield can response the X-ray emission and produce visible photons that can be observed by using the CCD camera and PMTs. Figure 3(d) shows the signals of PMTs that are produced by the runaway electrons. The FILD signals of runaway electrons [**Passive**, represented by fiber 20, as shown in Fig. 1(b)] in discharge 63333 is two orders in magnitude that of discharge 63348, for in discharge 63333 the detector is much closer (about 65 mm) to the plasma. The loop voltage decreases to 0.2 V when the current enters flat-top phase, and the runaway electrons and the FILD signals (represented by **Passive**) decrease to a very low level.

B. Effect of fast electrons on FILDs

The lower hybrid wave (LHW) is injected usually before the plasma current flat-top for driving the non-inductive current for steady-state tokamak operation in EAST, as shown in Fig. 4. The plasma current in Fig. 4(a) ramps up to 600 kA during 2.4 s. The heating power of LHW is injected at 1.5 s, as shown in Fig. 4(b). The co-current neutral beam left source (named NBI1L) is injected at 2.56 s with the energy of 60 keV in Fig. 4(c). The D_α in Fig. 4(d) indicates that the plasma converts to H-mode at 2.6 s. The Mirnov magnetic pickup coil signal is shown in Fig. 4(g). To evaluate the effect of fast electrons, the position of the detector is moved away from the plasma at the major radius of 2.368 m. The signal of the **Active** (fiber 7 usually used to represent the signals of lost fast-ions' region) is just as weak as the **Passive** (fiber 20 usually used to represent the signals of region without lost fast-ions) during the whole discharge, shown in Figs. 4(e) and 4(f), which means that the scintillator detector only collects the background signals of fast electrons.

Figure 4(I) is the enlarged view of discharge 62649 at the beginning of LHW injected. The background signals of the scintillator detector start increasing and then keep steady, for a number of thermal electrons are driven to fast electrons as the LHW is injected. Figure 4(II) is the zooming in of discharge 62649 during Type-I H-mode as the NBI1L is injected into the plasma. As the position of the FILD detector is too far from the plasma, the **Active** has no signals of lost fast-ions. The **Active** and **Passive** only collect the signals of fast electrons driven by LHW. The **Active** and **Passive** signals [Figs. 4(II-b) and 4(II-c)] both burst synchronous with the D_α emission. The **Active** and **Passive** signals have many fluctuations during the intermission of ELMs. The fluctuations are also found in the magnetic fluctuation, but not found in the D_α signal

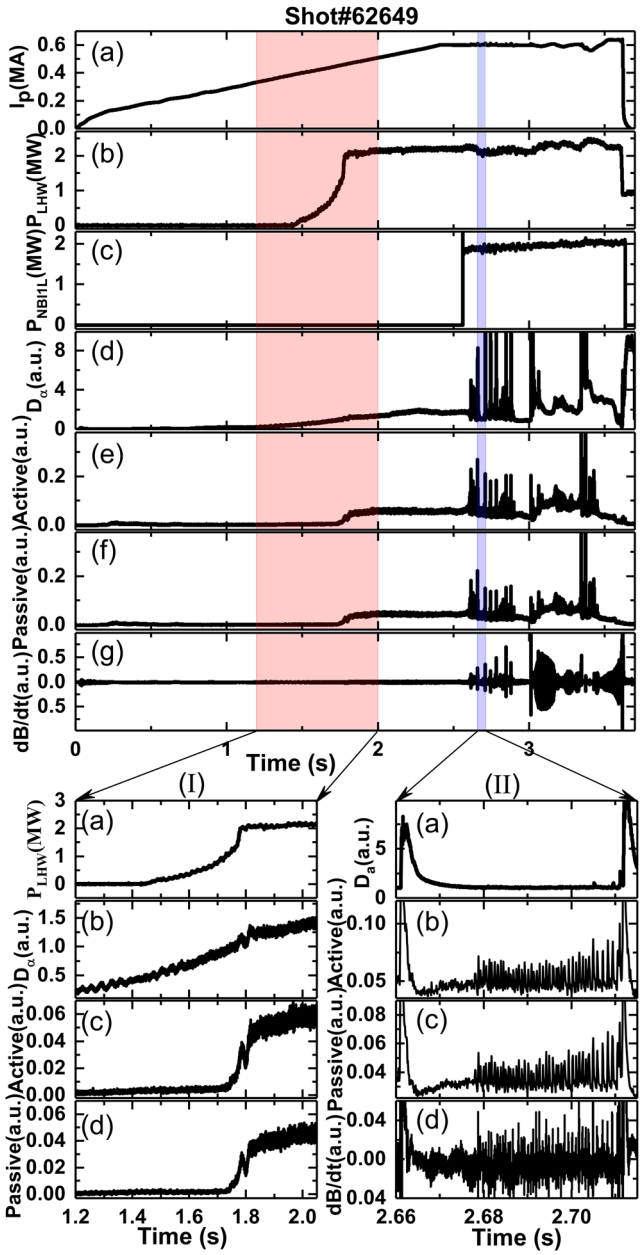

FIG. 4. EAST discharge 62649. Overview of discharge with (a) plasma current, (b) power of LHW, (c) power of NBI1L, (d) D_α, [(e) and (f)] scintillator screen signals (**Active** and **Passive**), and (g) the Mirnov magnetic pickup coil signal. The subfigure (I) shows time traces of (a) power of LHW, (b) D_α, (c) and (d) scintillator screen signals (**Active** and **Passive**). The subfigure (II) shows time traces of (a) D_α, (b) and (c) scintillator screen signals (**Active** and **Passive**), and (d) the Mirnov magnetic pickup coil signal intra-ELM.

[Fig. 4(II-a)]. In this regard, the fluctuations of scintillator screen signals between ELM bursts might be the result of electromagnetic perturbation in the edge.

The effective FILD signals can be acquired as the scintillator based detector is moved to a proper position. Figure 5 shows a typical EAST discharge of Type-III ELMy H-modes. The position of the FILD detector is away from the plasma at a major radius of R = 2.338 m in discharge 68972. The beam energy of co-current neutral beam left and right sources (named NBI1L and NBI1R) is 50 keV. The **Active** signal manifesting the first orbit losses of the neutral beam in Fig. 5(b) is much higher than the **Passive** signal in Fig. 5(c). The bursts

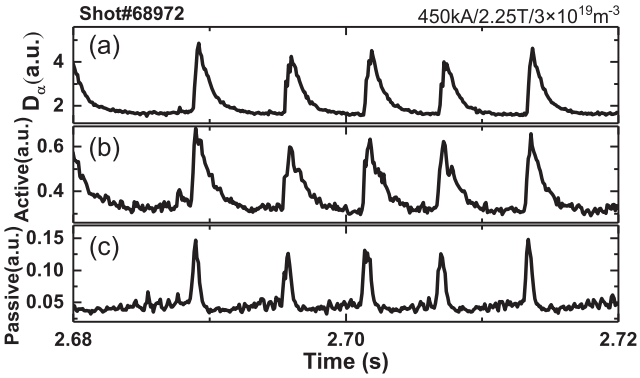

FIG. 5. Time traces of (a) D_α, (b) **Active** signal of FILD PMTs, and (c) **Passive** signal of FILD PMTs. The power of LHW is 2.4 MW, and the power of left and right co-NBI is 1.2 MW each.

of fast-ion losses are observed just as the ELM bursts, comparing with D_α emission in Fig. 5(a). These ELM-induced fast-ion losses are one order of magnitude higher than the signals of neutral beam prompt loss. The **Passive** signal shows the same trend with the **Active** signal, but the amplitude and decay time of **Passive** signals are much smaller than of **Active** signals. So the fluctuations of fast-ion losses in the **Active** signal are caused by ELM electromagnetic perturbation, while the fluctuations of the **Passive** signal are related to the perturbations and redistributions of fast electrons derived by ELMs. Since the signal caused by background fast electrons is much smaller than that of fast-ion losses, the background signal is negligible for studying the behavior of fast-ion losses.

V. SUMMARY

A FILD system equipped with a CCD camera and PMTs has been installed on EAST to study the behavior of fast-ion losses. By applying the rotatable platform, the beam-ion prompt loss can be measured in normal and reverse magnetic fields. To understand the interference on lost fast-ion signals, the effects of energetic electrons (including runaway electrons and fast electrons) on the scintillator-based detector have been studied. For runaway electrons produced in the plasma current ramping-up phase, the thick-target bremsstrahlung occurring in the stainless steel shield can produce X-rays which will strike on the scintillator based detector. In LHW discharges, the background signals caused by fast electrons do exist, but the amplitude is negligible compared with lost fast-ion signals. Considering the effect of the fast electron on the fast-ion lost signal, it is better to make more shielding such as carbon or ceramics material used for the detector head in the further improvement.

ACKNOWLEDGMENTS

This work was supported by the National Natural Science Foundation of China No. 11575249, National Magnetic Confinement Fusion Energy Research Program of China under Contract Nos. 2014GB109004 and 2015GB110005, and Hefei Science Center CAS (No. 2017HSC-IU005).

[1] M. García-Muñoz *et al.*, Rev. Sci. Instrum. **80**, 053503 (2009).
[2] S. J. Zweben *et al.*, Nucl. Fusion **30**, 1551 (1990).
[3] A. Werner *et al.*, Rev. Sci. Instrum. **72**, 780 (2001).
[4] D. S. Darrow *et al.*, Rev. Sci. Instrum. **79**, 023502 (2008).
[5] S. Baeumel *et al.*, Rev. Sci. Instrum. **75**, 3563 (2004).
[6] K. Ogawa *et al.*, J. Plasma. Fusion Res. Ser. **8**, 0655 (2009), available at http://www.jspf.or.jp/JPFRS/index_vol8-4.html.
[7] R. K. Fisher *et al.*, Rev. Sci. Instrum. **81**, 10D307 (2010).
[8] J. Kim *et al.*, Rev. Sci. Instrum. **83**, 10D305 (2012).
[9] Y. P. Zhang *et al.*, Rev. Sci. Instrum. **85**, 053502 (2014).
[10] J. F. Chang *et al.*, Rev. Sci. Instrum. **87**, 11E728 (2016).
[11] Z. Jin *et al.*, Fusion Eng. Des. **125**, 160 (2017).
[12] Z. Jin *et al.*, Nucl. Technol. **40**, 110605 (2017) (in Chinese with English abstract).
[13] R. J. Zhou *et al.*, Phys. Scr. **84**, 015501 (2011).